Empirical synthesis of time-asymmetrical Green functions from the correlation of coda waves

Anne Paul, Michel Campillo,[1] Ludovic Margerin, and Eric Larose

Laboratoire de Géophysique Interne et Tectonophysique, Observatoire de Grenoble, Université Joseph Fourier and CNRS, Grenoble, France

Arnaud Derode

Laboratoire Ondes et Acoustique, Université Paris 7 and CNRS, Paris, France

Received 4 November 2004; revised 21 March 2005; accepted 13 April 2005; published 5 August 2005.

[1] We demonstrate the existence of long-range field correlations in the seismic coda of regional records in Alaska. The cross correlations between the different components of coda records at two points are measured for a set of distant earthquakes. Remarkably, while individual correlations have a random character, the correlations averaged over source and time exhibit deterministic arrivals that obey the same symmetry rules as the Green tensor between the two points. In addition, the arrival times of these waves coincide with propagating surface waves between the two stations. Thus we propose to identify the averaged correlation signals with the surface wave part of the Green tensor. We observe the causal and anticausal parts of the Green function. However, we find experimentally that amplitudes at positive and negative times are not equal. We explain this observation by the long-lasting anisotropy of the diffuse field. We show that the flux of energy coming from the source can still dominate the late coda and result in nonsymmetric cross correlations when the distribution of earthquakes is not isotropic around the stations. The extraction of Green functions from coda waves allows new types of measurements with seismic waves along paths between stations that could not be obtained with the waves produced by earthquakes.

Citation: Paul, A., M. Campillo, L. Margerin, E. Larose, and A. Derode (2005), Empirical synthesis of time-asymmetrical Green functions from the correlation of coda waves, *J. Geophys. Res.*, *110*, B08302, doi:10.1029/2004JB003521.

1. Introduction

[2] Recent studies [*Lobkis and Weaver*, 2001; *Weaver and Lobkis*, 2001a, 2002] showed from laboratory experiments with ultrasonic and thermal noise that the Green function can be extracted from the correlation properties of random fields. In seismology, two kinds of fields are usually considered as random: the seismic noise and the scattered waves of the coda. The idea of using random noise to extract deterministic signals had already been proposed and had found spectacular applications in helioseismology [*Duvall et al.*, 1993; *Rickett and Claerbout*, 2000]. Seismic noise has the advantage to be easy to record and to exist even in regions without earthquakes. *Shapiro and Campillo* [2004] have shown that coherent broadband dispersive wave trains emerge from the cross correlation of ambient seismic noise records between stations many hundred kilometers apart and that dispersion curves can be measured in the absence of earthquake records. However, the question of the origin of seismic noise is still open. Without a clear understanding of the source of the seismic noise, the relevant propagation regime (ballistic, diffusive.) remains unknown. It is thus difficult to better understand the properties of the emergence of the Green function from diffuse wave fields using only noise records.

[3] In this paper, we concentrate on coda waves since they are produced by a known source, with precise location and origin time, and they have been shown to result from multiple scattering in the Earth lithosphere. *Campillo and Paul* [2003] showed that extracting the Green function from field-to-field correlation of scattered waves is a valid approach not only in the controlled and favorable conditions of the laboratory, but also with natural signals such as actual seismograms produced by earthquakes. They used coda waves produced by moderate earthquakes in Mexico. The part played by multiple scattering and diffusion in the coda of the seismograms has been a subject of discussion since the pioneering papers of *Aki* [1969] and *Aki and Chouet* [1975]. The importance of multiple scattering for the seismic coda is attested by the success of the use of radiative transfer theory to explain the observation of energy decay [*Abubakirov and Gusev*, 1990; *Hoshiba*, 1991; *Margerin*

[1]Also at Laboratoire de Physique et Modélisation des Milieux Condensés, Université Joseph Fourier and CNRS, Grenoble, France.

0148-0227/05/2004JB003521$09.00

et al., 1998, 1999]. Furthermore, the diffuse character of coda waves has been demonstrated by the observation of the stabilization of different energy ratios [*Campillo et al.*, 1999; *Shapiro et al.*, 2000; *Hennino et al.*, 2001], a phenomenon associated with the principle of equipartition in the phase space of a random field [e.g., *Weaver*, 1982]. Equipartition means that all the possible modes are excited at the same level of energy. In the present context, the word modes refers to all body waves or normal modes of surface waves that are potentially excited in the region probed by the diffuse field and can be coupled by local scattering. Equipartition is a property of diffuse elastic waves. It implies a stabilization of the ratio of S to P wave energy with time, independently of the source. It is an important point in the context of the present paper since it indicates that the modes which make up the Green function are represented in the diffuse field. In the following, we first summarize theoretical and experimental arguments that clarify the conditions for the emergence of the Green function from field correlations. We then present an application with data from a temporary broadband network in Alaska. Finally we discuss the role played by the source distribution and the time evolution of the wave field structure toward complete randomness.

2. Emergence of the Green Function and Multiple Scattering

[4] Contrary to ballistic waves, fully diffuse wave fields are expected to contain all possible modes and propagation directions following an equipartition principle. As explained above, this has been observed for coda waves through the stabilization of P to S energy ratio. Formally, an implication of the presence of all modes is that the information about any possible path is represented in the coda records. Mathematically, a wave field inside a finite elastic body can be expressed in modal form:

$$u(\mathbf{x},t) = \sum_n a_n \phi_n(\mathbf{x}) e^{i\omega_n t} \tag{1}$$

where $\mathbf{x}$ is position, t is time, ϕ_n is a convenient set of eigenfunctions, ω_n are eigenfrequencies, and a_n are modal excitation functions that depend only on the source. When disorder is added inside the body, after a sufficiently long time, the field becomes diffuse and a_n become random functions of time. Equipartition means that the modal amplitudes are uncorrelated random variables:

$$\langle a_n a_m^* \rangle = \delta_{nm} F(\omega_n) \tag{2}$$

where $F(\omega)$ is the spectral energy density of the source in the frequency band $[\omega - \delta\omega, \omega + \delta\omega]$. An implication of equation (2) is that all modes in a narrow frequency range are excited at the same energy level. The brackets in equation (2) mean either an ensemble average over the disorder or a time/frequency average of a single realization. Another type of average can be performed by considering a distribution of sources inside the body. In this case, a_n is a function of the location of the source and the bracket in (2) denotes a volume integral over source positions. The average correlation between the fields at locations x and y simply becomes

$$\langle C(x,y,\tau) \rangle = \sum_n F(\omega_n)\phi_n(\mathbf{x})\phi_n(\mathbf{y}) e^{-i\omega_n \tau} \tag{3}$$

since the cross terms disappear on average owing to (2).

[5] Expression (3) differs only by an amplitude factor F from an actual Green function between points $\mathbf{x}$ and $\mathbf{y}$. A very important implication of this result is that the Green function between two locations (or at least, the arrival times of the different wave trains) can be extracted from the diffuse field with a simple field-to-field correlation averaged either over a sufficiently long time or an extended enough source distribution.

[6] *Weaver and Lobkis* [2001a] exposed the above arguments and showed in laboratory experiments that the appropriately filtered average cross correlation of the fields at two positions is the Green function between the two points. The same arguments hold for an open medium as well [*Weaver and Lobkis*, 2004]. Under the assumption of complete randomness of the wave field, *Snieder* [2004] gave a ray geometrical interpretation of the reconstruction.

[7] Arguments such as those above which depend on assumptions of well developed diffuse fields are perhaps problematic for application to seismology because the distribution of earthquakes is discrete and uneven. Furthermore, the duration of available time series is limited by dissipation and ambient noise. Field fluctuations are expected that appear in the correlation function as a noise superimposed onto the expected deterministic signal. Small energy arrivals will emerge only after a very long averaging. In practical applications with the type of data available, we therefore expect to reconstruct only the more energetic parts of the Green function.

[8] Laboratory experiments with ultrasound and numerical simulations help to investigate the possibility of reconstructing the Green function in conditions close to those encountered in seismology. *Derode et al.* [2003a, 2003b] proposed an interpretation of the emergence of the exact Green function from the cross correlation of the fields received by two passive sensors in a heterogeneous medium. Their argument is based on an analogy of the averaging of a cross-correlation function over a series of sources with a physical operation of time reversal that can be performed in the laboratory [*Fink*, 1992; *Wu et al.*, 1992]. The operation of cross correlation of the signal produced by a source in S at receivers in A and B is formally equivalent to having a source in A producing waves recorded in S, time-reversed and reemitted from S to be recorded in B [*Derode et al.*, 2003a]. This last operation is exactly what is realized in a time-reversal mirror. This analogy shows how cross correlation is related to the physical wave propagation.

[9] We illustrate this point with numerical simulations conducted in a two-dimensional (2-D) acoustic medium. This configuration is chosen because it is a simple way to describe wave propagation at the surface of the Earth. We solve the wave equation using a finite difference code [*Tanter*, 1999; *Derode et al.*, 2001]. The field produced by each of several sources S is computed at each point of the medium. We consider a weakly scattering medium, where the distance of propagation is smaller than the transport

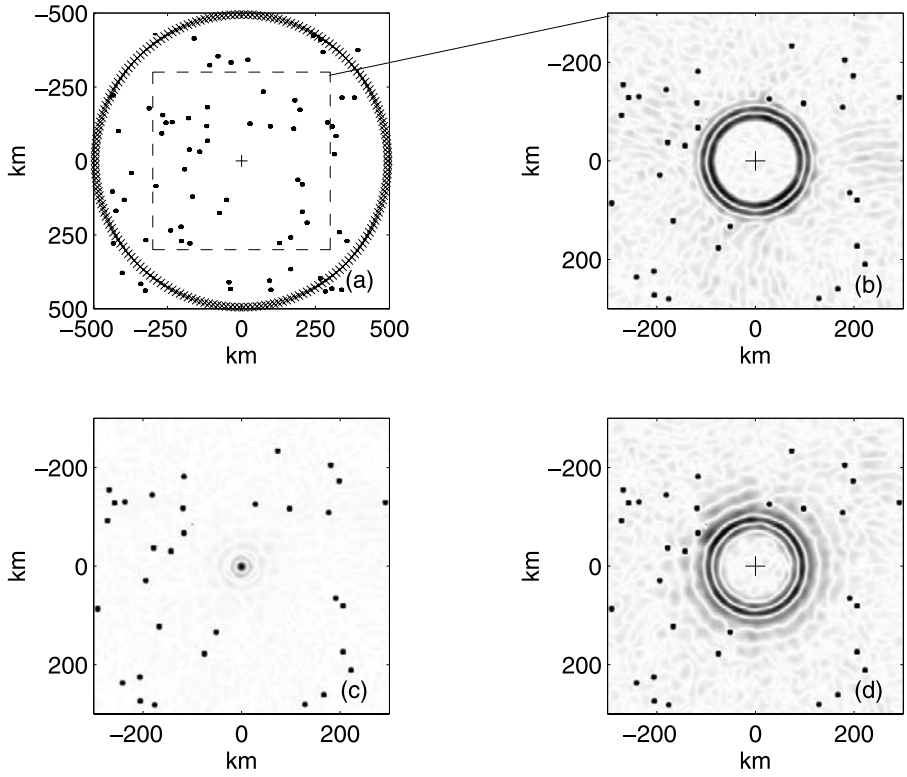

Figure 1. Numerical simulation of the reconstruction of the causal and anticausal parts of the Green function from cross correlations. (a) Configuration of the numerical experiment. One thousand sources S ($\times$) are surrounding the reference point A (pluses). Dots indicate the point scatterers. (b) Snapshot of the cross correlation between the field in A with the field at location (x, y) after averaging over the sources S for correlation time −30 s. The weakly diffusive medium is characterized by the transport mean free path l^* = 640 km, which is larger than the distance between the points where the correlations are computed. A converging wave front is well defined and constitutes the anticausal part of the Green function. (c) Snapshot for correlation time t = 0 s. The wave front is focused on A. (d) Snapshot for t = 30 s. The diverging wave front corresponds to the causal part of the Green function.

mean free path of the waves. We recall that the transport mean free path l^* is the typical distance after which the scattered energy of a wave in a particular direction is spread over all directions. The scattering is caused by a distribution of small rigid scatterers with radius a. The background velocity is 3.3 km.s^{-1}. The product of the wave number k by the radius a equals 1. Following the time-reversal analogy developed by *Derode et al.* [2003a], we choose to place the sources S all around A (the reference point at the center of the grid marked with a cross in Figure 1a) in order to form an equivalent of a perfect time reversal mirror. This configuration is depicted in Figure 1a. Each source S sends a broadband pulse with 0.1 Hz central frequency. The correlations are computed between the field $h_{SA}(t)$ at the reference point A and the field $h_{SR}(t)$ at any other point $R(x, y)$ of the grid. The correlation is averaged over the entire set of sources S. The wave field reconstructed by correlations is displayed in Figure 1 for correlation times −30, 0, and 30 s. Time t = 0 is the central time of the correlations, when all the energy is focused in A as if A was a source. At negative times, we observe a converging wave front, and a diverging wave front at positive times. These wave fronts correspond to the causal (positive times) and anticausal (negative times) parts of the Green function between A and any point R in the medium. The nearly perfect reconstruction of the Green function (including the converging and diverging wave fronts) is due to the quasi-ideal distribution of sources around A, the length of the coda (as long as allowed by the numerical schemes: 200 oscillations) and the absence of absorption. This numerical experiment shows that cross correlation corresponds to a physical process and is not an artifice of signal processing.

[10] *Derode et al.* [2003b] and *Larose et al.* [2004] showed the role of multiple scattering in enhancing the efficiency of the reconstruction of the Green function with a limited number of sources and finite durations of recording, in conditions closer to seismology. Since in seismology, the duration of records is limited by the presence of noise and by absorption, averaging over a set of different sources is required to expect the emergence of the Green function. The limitations of the reconstruction will be discussed in section 3 after an application of this simple principle to a data set of actual seismograms.

3. Application to Coda Records

3.1. Data Processing

[11] Temporary networks of seismic stations installed in regions with a high level of seismicity provide useful data sets to study the properties of the emergence of Green

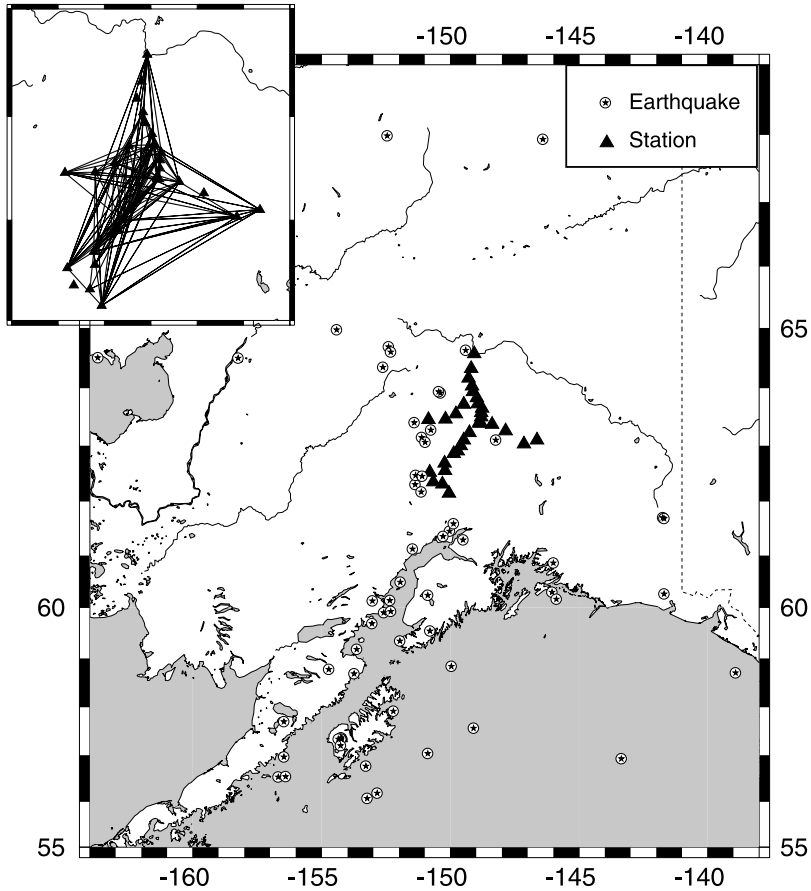

Figure 2. Map of stations and earthquakes. The paths between couples of stations for which average cross correlations have been computed are shown in inset.

functions from the correlations of coda waves. They include numerous stations with identical instrument characteristics that make it possible to compute cross correlations between many station couples separated by a large range of distances and with different orientations. Time-distance seismic sections can be constructed from the correlation signals where the propagating waves can be easily identified even with a poor signal-to-noise ratio. Actually, only limited averaging can be performed with coda records, and the deterministic signal is mixed with the remnant random fluctuations of the diffuse field.

[12] We present here an application of the extraction of Green functions from coda waves to the data of a temporary network in Alaska. During the Broadband Experiment Across the Alaska Range (BEAAR), a network of 36 broadband seismographs was operated during 2.5 years ending in August 2001 [*Ferris et al.*, 2003]. Most stations recorded simultaneously about 100 regional earthquakes with magnitude larger than 3.3. Locations of stations and epicenters are shown in Figure 2.

[13] Note that the distribution of earthquakes is not even and that they are mostly concentrated to the southeast of the network. The broadband seismograms were first band-pass filtered. For each couple of stations, the horizontal components of the seismograms were rotated assuming the interstation great circle path to be the radial direction. We used coda records starting 20 s after the arrival of the *S* wave and ending when the signal-to-noise ratio was smaller than 4. An example of record is shown in Figure 3. Because of the exponential decrease of coda amplitude with time, we cannot perform a simple cross correlation between the coda signals recorded at the two stations without strongly overweighing the earliest part of the coda.

[14] To avoid this problem, we followed *Derode et al.* [1999] by disregarding the amplitudes completely and considering only one-bit signals. *Campillo and Paul* [2003] checked that this procedure leads to the same results as compensating for amplitude attenuation with time in successive time windows. For each couple of stations, the cross correlation of one-bit signals was computed for each earthquake, normalized to a maximum amplitude of one, and averaged over the entire set of events. This processing was performed for all combinations of components, such as vertical to vertical (Z/Z), vertical to transverse (Z/T), radial to radial (R/R), etc. The results of *Campillo and Paul* [2003] suggest that these different field-to-field correlations contain the different terms of the elastic Green tensor. *Wapenaar* [2004] demonstrated the retrieval of the elastic Green tensor from surface displacement fields produced by a distribution of sources on a closed surface in the medium. Even if the source distribution does not fulfill such a condition in actual experiments, he gives a firm theoretical argu-

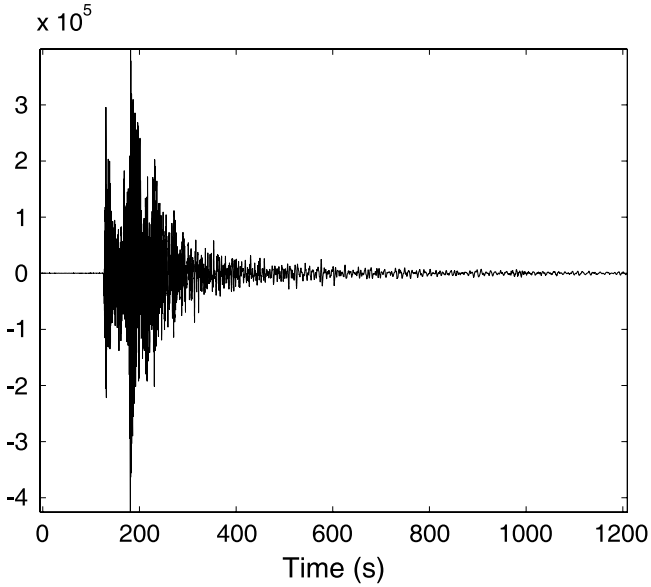

Figure 3. Example of broadband record from a regional earthquake. Note that the signal remains well above the noise level for several hundreds of seconds after the *S* wave arrival.

ment for the reconstruction of the polarized elastic response.

3.2. Results

[15] Figure 4 shows the results of the processing in the frequency band 0.08–0.3 Hz. The nine polarization combinations correspond to the terms of the Green tensor, that is for example the R/Z correlation corresponds to the vertical displacement produced by a force in the radial direction. Since we disregard the amplitudes of the coda waves by using one-bit signals, the relative amplitude of the reconstructed signals between the components is lost. Traces with a maximum amplitude at negative time have been time reversed to concentrate the large-amplitude pulses at positive times and have a better view of the presence, or the absence, of symmetry in time. Note that the location of the maximum amplitude pulse at positive or negative times only depends on the order of the signals in the cross correlation, which is arbitrary. Clear propagating wave trains can be observed on the Z/Z, Z/R, R/Z, R/R, and T/T components. The Z/T, R/T, T/Z, and T/R components only contain noise, as expected from the symmetries of the Green tensor. Figure 4 confirms the conclusions of *Campillo and Paul* [2003] for numerous paths with different azimuths. When a propagating branch can be seen at positive times, a symmetric one is more or less clearly visible, depending on the component, at negative times. This symmetric wave train is particularly clear on the Z/Z and T/T components at short offsets. We discuss the question of the time symmetry in more details in section 4.

[16] To test the reliability of the extraction of the Green function from the data, we computed synthetic Green functions in a 1-D velocity model derived from the seismic profiles recorded by *Beaudoin et al.* [1992] in the neighbor Tanana terrane. The computations are performed for a vertical point source acting at the free surface. The receivers are also at the free surface in a configuration similar to our station-to-station measurements. The synthetic section in the frequency band 0.08–0.3 Hz is shown in Figure 5 in the same distance range as in Figure 4. It is dominated by low-frequency surface waves (Rayleigh waves in this case), as the cross-correlation records. As expected for a point force source at the free surface, the body wave contributions to the Green functions are negligible. We performed the same computation in a frequency band centered on 1 Hz (Figure 5). The surface waves still dominate. This argument based on a flat-layered structure must be moderated by the fact that surface waves at these frequencies are strongly diffracted by topography and shallow structures which are neglected in the 1-D model. It is nevertheless a good indication that the assumption that the prominent arrivals in the actual surface/surface Green function are surface waves is reasonable for the frequency and distance ranges considered here.

[17] The reconstructed arrivals can be observed at distances as large as 200 km, confirming the existence of strong long-range correlations in coda waves. As already observed by *Campillo and Paul* [2003], and demonstrated by the comparison with synthetics, the dominant signals correspond to the fundamental Love and Rayleigh waves. A simple phase velocity measurement on the Z/Z and T/T components of Figure 4 confirms that the velocities of the prominent wave trains are in a good agreement with the expected dispersion curves of Rayleigh and Love waves in the simple model derived from *Beaudoin et al.* [1992]. The signal-to-noise ratio decreases with increasing distance. This is a natural consequence of the spatial decay of the Green function. The deterministic signal decreases rapidly while the physical fluctuations of the diffuse fields remaining after partial averaging are independent of the epicentral distance. We assume here that the fluctuations are proportional to the square of the amplitude of the diffuse field. This amplitude is known to vary weakly with distance in the diffuse regime. It has been shown to be almost independent of distance for the late coda [e.g., *Lacombe et al.*, 2003, Figure 3]. These observations suggest that even amplitude characteristics could be reconstructed from field correlations. However, a reliable measurement of the amplitude decay with distance would require that the same set of earthquake records and time windows are used for all the couples of stations. It is not the case here since all stations were not operating exactly at the same time.

[18] We are only able to reconstruct the surface waves because the Green function is expected to be dominated by surface waves. A high level of noise remains after the limited averaging we performed. It prevents an unambiguous identification of body waves. The reconstruction of the high frequencies is difficult because absorption limits the durations of the available coda records. These limitations could be overcome with a larger data set.

4. Time Symmetry and Isotropy of Diffuse Wave Fields

4.1. Observations

[19] In Figure 4, we have arbitrarily chosen the direction of time so that the maximum amplitude of the average cross

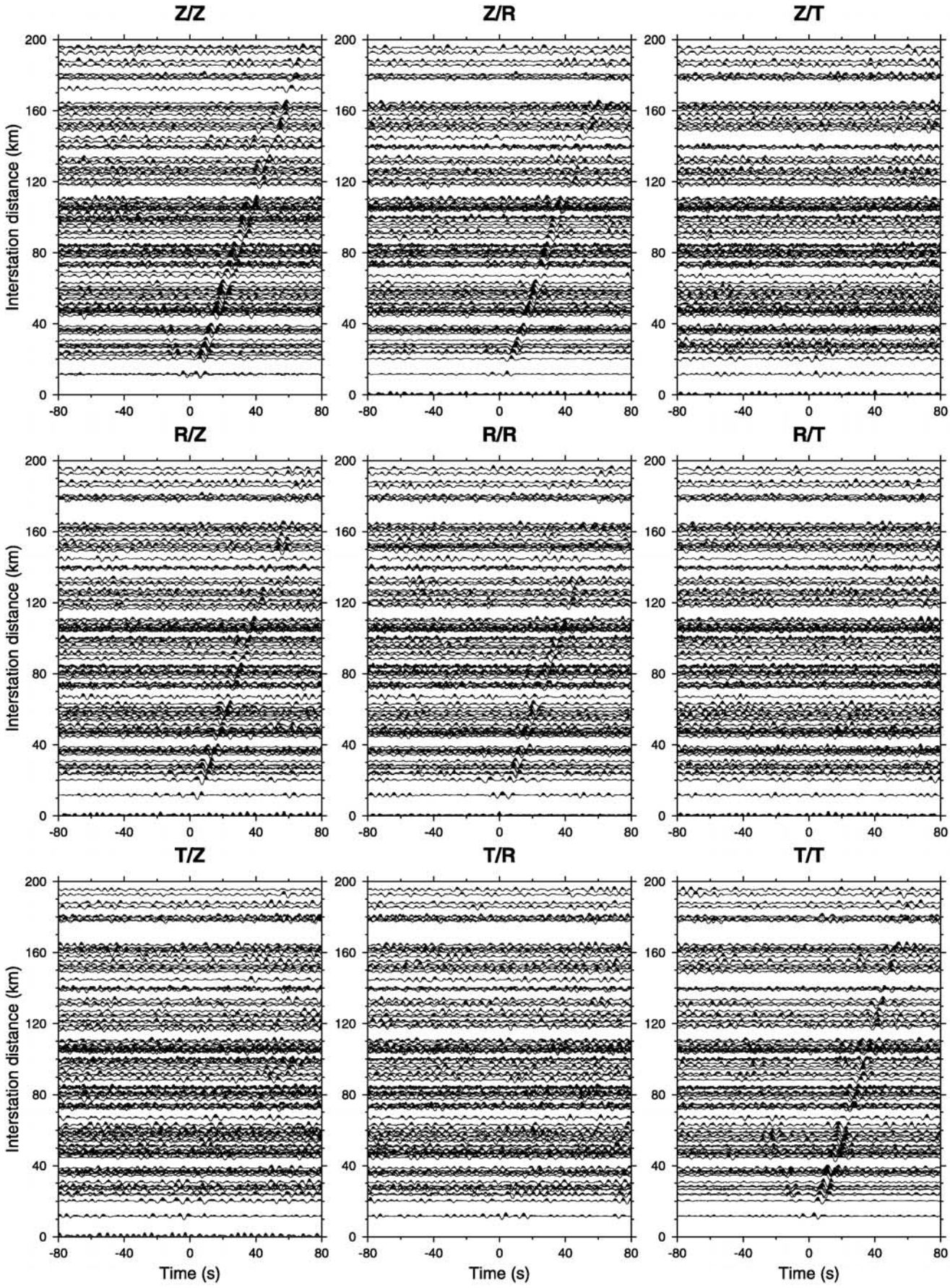
Z/Z
Z/R
Z/T
R/Z
R/R
R/T
T/Z
T/R
T/T
Interstation distance (km)
Time (s)
0
40
80
120
160
200
-80
-40
0
40
80

Figure 4

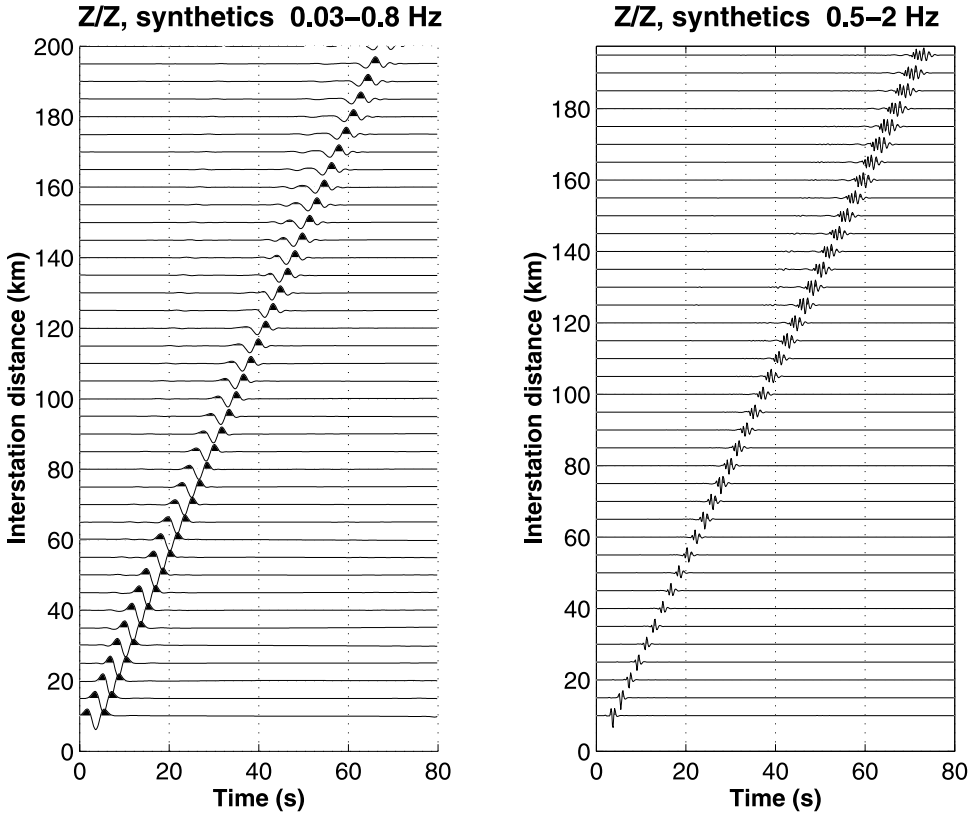

Figure 5. Synthetic vertical seismograms for source and receivers at the free surface in a flat-layered crust. The source is a vertical force. Two different frequency bands are considered. Note the prominence of the Rayleigh waves.

correlation is at a positive time. Swapping the two stations in the cross correlations gives a time series which is exactly the time reversed of the original by definition of cross correlation. Since the identification of the waves only relies upon the variations of the travel time with distance, this choice has no consequence. On the other hand, Figure 4 exhibits a strong asymmetry of the cross-correlation time functions. One must remember that theoretically we expect to see both causal (retarded) and anticausal (advanced) parts of the Green function. Nevertheless we observe that for most station couples, a single direction of time is favored. A similar observation was made by *Campillo and Paul* [2003] in Mexico. They used earthquakes along the subduction and found that the cross-correlation functions are asymmetrical for stations inland with an orientation perpendicular to the coast and symmetrical for stations located along the coast within the earthquake source region. They suggested that time asymmetry indicates a preferential direction of flow of the energy of coda waves, a property that could appear as paradoxical in the context of random fields. In the following, we will discuss this issue in relation with multiple scattering and the uneven distribution of epicenters which are mostly located to the southeast of the network in Alaska.

[20] Let us consider the Z/Z correlation profile of Figure 4. Using different bandpass filters, we attempted to see whether the level of asymmetry varies with frequency or not. However, the signal-to-noise ratio does not allow any convincing visual comparison. To achieve a more quantitative analysis, we performed a slant stack of the cross correlations. For each trace, the arrival time of the Rayleigh wave was measured in the positive times, where by construction the largest amplitude is found. We then shifted the traces of the time of the maximum and stacked all the arrivals in the positive times. We stacked the signals in the negative times in the same way using time shifts opposite to the ones measured in the positive times. This operation enhances the coherent arrivals and takes into account the variations of wave velocity among the different paths. Finally we computed the ratio between the maximum amplitude of the stacked Rayleigh pulses in the positive time to the maximum amplitude of the stack in the negative time. The stacks were performed for all traces corresponding to interstation distances between 20 and 120 km which have the best signal-to-noise ratio. This processing was applied to the sections of the Z/Z correlation profile of Figure 4 after band-pass filtering. We obtained an amplitude ratio of 3.8 in the band 0.12–0.3 Hz and 4.0 in the band 0.08–0.15 Hz indicating that the symmetry is slightly stronger for high frequency. However, we also expect the late coda to behave differently from the early

Figure 4. Average cross correlations as a function of interstation distance. The correlations have been computed for every combination of components of motion, vertical (Z), radial (R), and transverse (T).

coda. Because of anelastic absorption, the early coda includes more high frequencies. As a consequence, the influences of both lapse time and frequency on the symmetry are mixed up in this analysis when we consider cross correlations computed on the whole coda length.

[21] To clarify this point, we studied the dependence of the causal to anticausal amplitude ratio with the lapse time in the coda window. We formulate as a first-order hypothesis that the larger the lapse time, the more isotropic the coda. According to this argument, we expect the correlations computed in later time windows to be more symmetric in time since the corresponding diffuse wave field is more isotropic and all directions of propagation are closer to be equally represented. To verify the reality of this effect, we compared the amplitude ratio of positive and negative times for correlations computed for different lapse times and the same two frequency bands as before. We considered first the correlations computed from the first 300 s of coda (early coda) filtered in the low frequency band (0.08–0.15 Hz). We found a ratio of stacked amplitudes of 5.6. We repeated the measurement for correlations computed from record windows starting 300 s after the beginning of the coda (late coda). The amplitude ratio between the causal and anticausal signals is 3.9. This indicates that the correlations are more symmetrical when measured from the late coda than from the early coda. In other words, the longer time the scattered waves propagate, the more isotropic they are. We performed the same analysis in the band 0.12–0.3 Hz. For the early coda the amplitude ratio is 4.3, while it is 3.1 in the late coda. This confirms that the pulses emerging from the cross correlations of the late coda are more symmetric in time than those computed from the early coda. Comparing ratios obtained in the two frequency bands, we find that the values are smaller for the band 0.12–0.3 Hz than for 0.08–0.15 Hz. This indicates that the high-frequency waves are evolving faster toward isotropy. In the following, we investigate theoretically and from numerical simulations what is the expected evolution of the net flux of energy with time along a seismogram and if this evolution accounts for the observations.

4.2. Multiple Scattering and Isotropy

[22] In this section, we discuss quantitatively the impact of the anisotropy of energy flux on the time asymmetry of the Green function recovered by cross correlations. For sake of simplicity, we consider the theory for scalar waves. The results are not expected to be different for the energy of elastic waves as it will be discussed later. The angular distribution of energy at position $\mathbf{R}$ and time t is described by a specific intensity $I_{\mathbf{R}}(\hat{p}, t)$ defined as the energy flux in space direction $\hat{\mathbf{p}}$ per unit solid angle. The specific intensity is the solution of a radiative transfer equation, which can be derived from an ensemble average of the wave equation [*Weaver*, 1990; *Ryzhik et al.*, 1996]. The radiative transfer equation is a local detailed energy balance which describes the transport of energy through a multiple scattering medium. In general, it is an integrodifferential equation that can only be solved numerically. However, after many scattering events, the initial distribution of energy in phase space tends to be homogenized, which implies that the angular dependence of the specific intensity departs only slightly from isotropy. When this assumption is valid, I can be expanded as follows:

$$I_{\mathbf{R}}(\hat{\mathbf{p}}, t) = \frac{1}{4\pi}[\rho(\mathbf{R}, \tau) + 3\mathbf{J}(\mathbf{R}, \tau) \cdot \hat{\mathbf{p}} + \cdots] \tag{4}$$

where ρ denotes the energy density, and $\mathbf{J}$ is the energy current vector which points in the direction of maximum energy flow. The dots denote higher-order multipoles that are neglected. Equation (4) forms the basis of the diffusion approximation, which should apply at $t \gg \tau^\star$, where $\tau^\star$ denotes the transport mean free time. We introduce the "ideal" field-to-field correlation function C between two stations located at $\mathbf{R} + \mathbf{r}/2$ and $\mathbf{R} - \mathbf{r}/2$:

$$C_{\mathbf{R}}(\mathbf{r}, \tau) = \int_{-\infty}^{+\infty} u(\mathbf{R} + \mathbf{r}/2, t + \tau/2)u^\star(\mathbf{R} - \mathbf{r}/2, t - \tau/2)dt \tag{5}$$

where $\mathbf{R}$ represents the mean distance between source and stations and $\mathbf{r}$ the interstation distance. The diffusion approximation can be used to derive an asymptotic ($t \rightarrow \infty$) relation between C and the ensemble average Green function of the medium [*van Tiggelen*, 2003]:

$$C_{\mathbf{R}}(\mathbf{r}, \tau) = \rho(\mathbf{R}, \tau)\frac{\partial}{\partial \tau}[\langle G_B(\mathbf{r}, \tau)\rangle - \langle G_B(\mathbf{r}, -\tau)\rangle] - 3\mathbf{J}(\mathbf{R}, \tau) \cdot \nabla[\langle G_B(\mathbf{r}, \mathbf{t})\rangle - \langle G_B(\mathbf{r}, -\tau)\rangle] \tag{6}$$

[23] In (6) brackets $\langle\cdot\rangle$ denote an ensemble average, and G_B is the retarded causal Green function filtered in frequency band B. Equation (6) applies to ensemble averaged quantities only, and is therefore not expected to apply strictly in the seismological case. However, it establishes a relatively simple relation between the field-to-field correlation function from a single source and partial derivatives of the (time-symmetric) Green function. It can be inferred that the partial derivatives $\partial\tau$ and $\partial_{\mathbf{r}}$ acting on the brackets $[\cdot]$ yield even and odd functions of time, respectively. Thus, as long as the dipolar (J) and isotropic (ρ) terms are of the same order, a time asymmetry is expected to persist.

[24] In the diffusive regime, the energy density is the solution of a simple diffusion equation:

$$\partial_t \rho(\mathbf{R}, t) - D\nabla^2\rho(\mathbf{R}, t) = \delta(t)\delta(\mathbf{R}) \tag{7}$$

and is related to the energy current by Fourier's law:

$$\mathbf{J}(\mathbf{R}, t) = -D\nabla\rho(\mathbf{R}, t) \tag{8}$$

D is the diffusion constant of the waves and is related to the transport mean free time $\tau^\star$ as follows:

$$D = v^2\tau^\star/3 \tag{9}$$

In equation (7) the delta functions represent idealized source terms for small earthquakes. Note that equations (7) and (8) are valid for coupled elastic waves. In that case, ρ must be interpreted as the sum of P and S energy densities and relation (9) takes a more complex form [*Turner*, 1998]. For

scalar waves in a simple infinite scattering medium with homogeneous background, the diffusion equation is easily solved, and the ratio Γ between the causal and anticausal parts of the correlation function can be written as [*Malcolm et al.*, 2004]:

$$\Gamma(\mathbf{R},t) = \frac{1+3R/2vt}{1-3R/2vt} \tag{10}$$

This relation is easily obtained by noting that $J/\rho = R/2t$ and $\partial_r = v\partial_\tau$ for a propagating wave of the general form $h(t - R/v)$. Equation (10) shows that for a single source the convergence of the ideal correlation function toward time symmetry is algebraic, of order t^{-1} only. This result has to be used with some caution since it relies on the assumption that the angular dependence of the specific intensity can be described by equation (4).

[25] To assess the range of validity of this expansion, we solved numerically the full elastic radiative transfer equation using the Monte Carlo method of *Margerin et al.* [2000]. Our analysis is limited to elastic body waves in an infinite space. The code previously developed to evaluate energy densities has been adapted to calculate the angular distribution of flux. Numerical solutions of the transport equations and analytical results of the diffusion approximation are shown in Figure 6. The medium is composed of spherical inclusions with slight (5%) deviations of density, and P and S velocities from the homogeneous background. The product of shear wave number and sphere radius is $k_S a \approx 2$. The scattering mean free time of shear waves is roughly 8 s and the detector is located 80 km away from a point-like shear source. Figure 6a demonstrates the rapid mixing of P and S modes. After about 50 s (six mean free times), the P to S energy ratio has stabilized. However, Figure 6b shows that the energy flux is strongly anisotropic at the same lapse time: the ratio between forward and backward fluxes is still larger than 4. It is therefore important to carefully make the distinction between the stabilization of the P to S energy ratio, the validity of the diffusion approximation, and equipartition.

[26] In the equipartition regime, all directions of propagation and all polarizations are supposed to be equally represented. Under these condition, the theoretical value of energy ratio $\beta^3/2\alpha^3$ (where β and α denote the shear and compression velocities) can be obtained from a simple mode counting argument [*Weaver*, 1982]. Note that this result is only valid for a full homogeneous open space and can be generalized to the case of the half-space [*Weaver*, 1985; *Hennino et al.*, 2001]. Figure 6 shows that the anisotropy of the field remains at very large times and therefore that equipartition occurs asymptotically ($t \to \infty$). On the contrary, the P to S energy ratio stabilizes at the theoretical value $\beta^3/2\alpha^3$ for a finite time. At this stabilization time, the diffusion approximation wrongly predicts both energy density and flux anisotropy. After about 100 s, radiative transfer and diffusion theory agree extremely well but the residual anisotropy of intensity is still of the order of 2 and decays algebraically as predicted by equation (10). The total energy density is correctly predicted by the diffusion approximation only when the dipolar term describes with sufficient accuracy the anisotropy of the specific intensity. The calculations prove: (1) that the stabilization of the P to S energy ratio is a rapid phenomenon; (2) that it does not imply isotropy of the wave field; (3) that the diffusion approximation may largely underestimate the anisotropy of the energy flux, even in the multiple scattering regime. It is important to notice here that formal equipartition would imply perfect isotropy (all modes, i.e., directions, equally represented). The stabilization of the P to S ratio occurs before the equipartition which is the asymptotic behavior of diffuse waves for large times. Therefore one may expect large time asymmetries of the field-to-field correlation functions as shown by equation (10), provided the sources are located in the same distant region. The asymmetry is expected to disappear both in the average cross correlations of late coda signals, or with an isotropic distribution of sources around the seismic network. In the latter case, each source produces an asymmetric correlation function but the antisymmetric terms from many sources are expected to average out.

[27] We return to the numerical experiments with the wave equation to illustrate the effect of a nonhomogeneous distribution of sources. The conditions of computation are similar to those used to produce Figure 1, but we now consider a configuration which mimics a set of earthquakes along a fault. 40 sources S are aligned in the x axis direction along a 400-km-long segment located 450 km away from the receivers as depicted in Figure 7. We use the same weakly scattering medium as in Figure 1. Snapshots of the correlation function are presented in Figure 7b for time $t = -30$ s, Figure 7c for $t = 0$ s, and Figure 7d for $t = 30$ s. For $t < 0$, the wave front is only reconstructed in the direction of the sources S, corresponding to the anticausal part of the Green function. For $t > 0$, only the causal part of the Green function is reconstructed in the region opposite to the sources.

[28] This numerical experiment confirms that the spatial distribution of the sources controls the time symmetry of the correlations. If the source distribution is asymmetric, the time symmetry of the correlations can be broken. This is particularly true in weakly scattering (or homogeneous) media. This can be understood as well in terms of the time-reversal analogy. The uneven distribution of earthquakes in a limited region has a similar effect as a limited aperture of a time-reversal mirror.

[29] At long lapse time, the field becomes diffuse and the argument given above (equation (10)) holds. We therefore expect that even with a inhomogeneous distribution of sources, scattering restores the broken time symmetry of the correlations. We checked this expectation with the same numerical experiment as before, but we correlated only the waves of the late coda. Late times in the coda are defined as $t > t^*$, where t^* is the mean free time, that is the mean free path divided by the velocity. After t^*, the waves have traveled more than l^* and the field is evolving toward isotropy. The result is shown in Figure 8a and proves that the time symmetry of the correlations is restored by using large enough lapse times. As a consequence of the discussion above on the isotropization of the field, we expect stronger scattering to improve the reconstruction of the Green function even for an inhomogeneous distribution of sources. This effect was already confirmed by laboratory experiments [*Derode et al.*, 2003b]. We performed numerical simulations in a

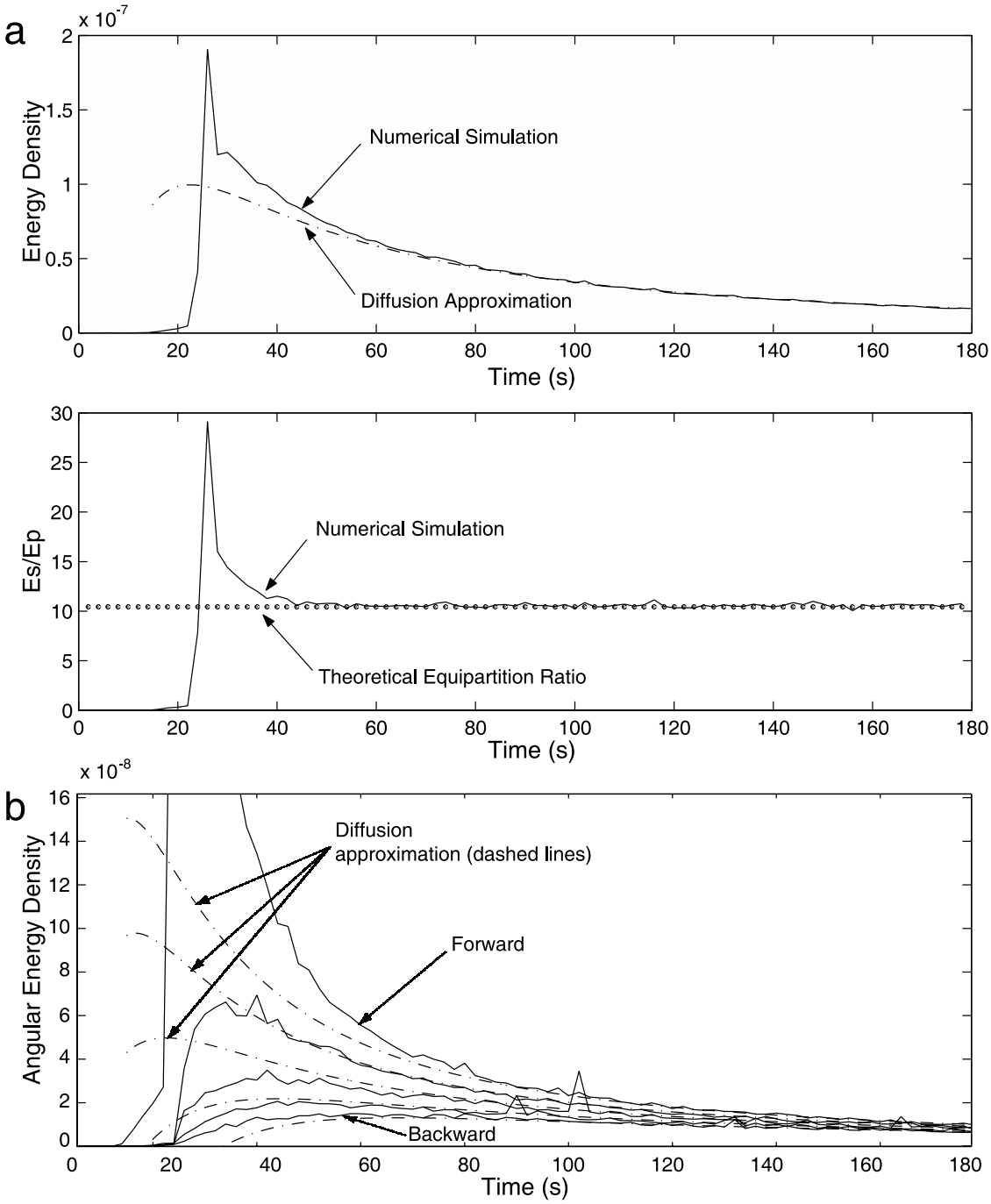

Figure 6. Comparison between numerical (Monte Carlo) solutions of the radiative transfer equation, and analytical solutions of the diffusion equation. (a) (top) Energy density and (bottom) P to S energy ratio. (b) Angular distribution of elastic energy flux. The dashed and solid lines show the results of the diffusion approximation and radiative transfer equation, respectively. The energy flux decreases monotonically from $\theta = 0$ (forward direction) to $\theta = \pi$ (backward direction), where θ denotes the angle between the propagation direction and the source-observer vector. The results for $\theta = \pi/4$, $\pi/2$ and $3\pi/4$ are also plotted.

strongly scattering medium (Figure 8b) and processed the complete coda window. Again, the converging wave front is clearly symmetric despite the uneven distribution of sources, unlike what we observed in the same conditions of computation with a weakly scattering medium (Figure 7).

[30] In our experiments on real earthquake records in Alaska, we observed a clear temporal asymmetry of the cross-correlation functions (Figure 4). It shows that the forward flux dominates and that the excitation of the propagation modes that make up the diffuse field is anisotropic. Indeed the earthquakes we used are concentrated

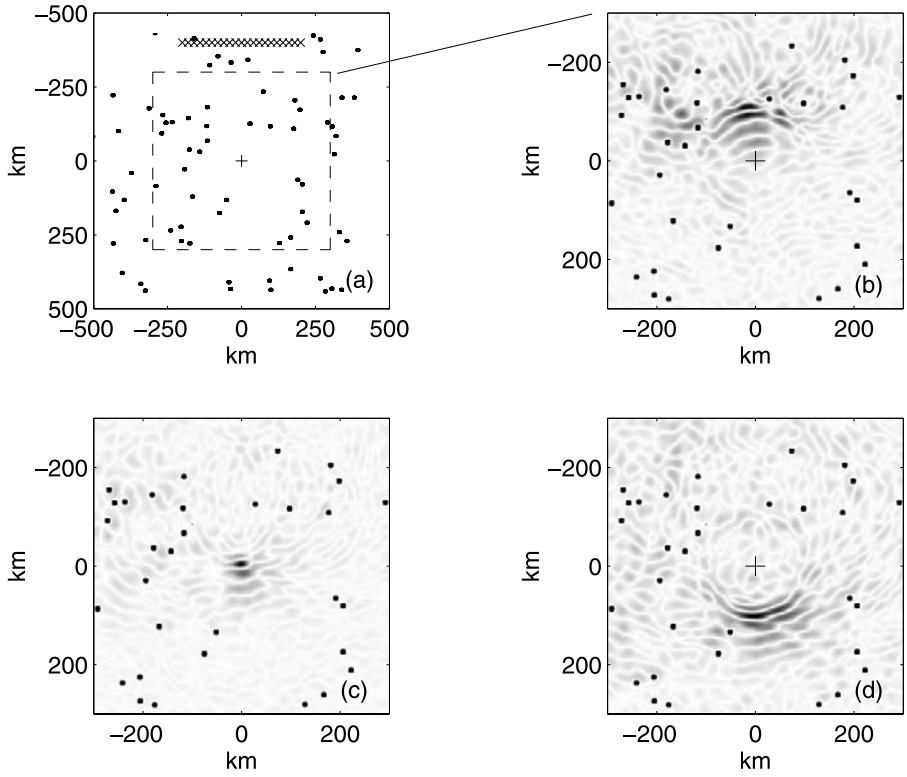

Figure 7. Numerical simulation of the asymmetry of the reconstructed Green function. (a) Forty sources S aligned along the x axis (crosses). The reference point is at the center of the plot, indicated by a plus. (b) Snapshot of the cross correlation between the field in A with the one at location (x, y) after averaging over the sources S for correlation time −30 s. The converging wave front is only partially reconstructed in the direction of the sources. (c) Snapshot for correlation time $t = 0$ s. The wave front is focused on A. Note the high level of remaining fluctuations. (d) Snapshot for $t = 30$ s. The diverging wave front is defined only in the direction opposite to the source region.

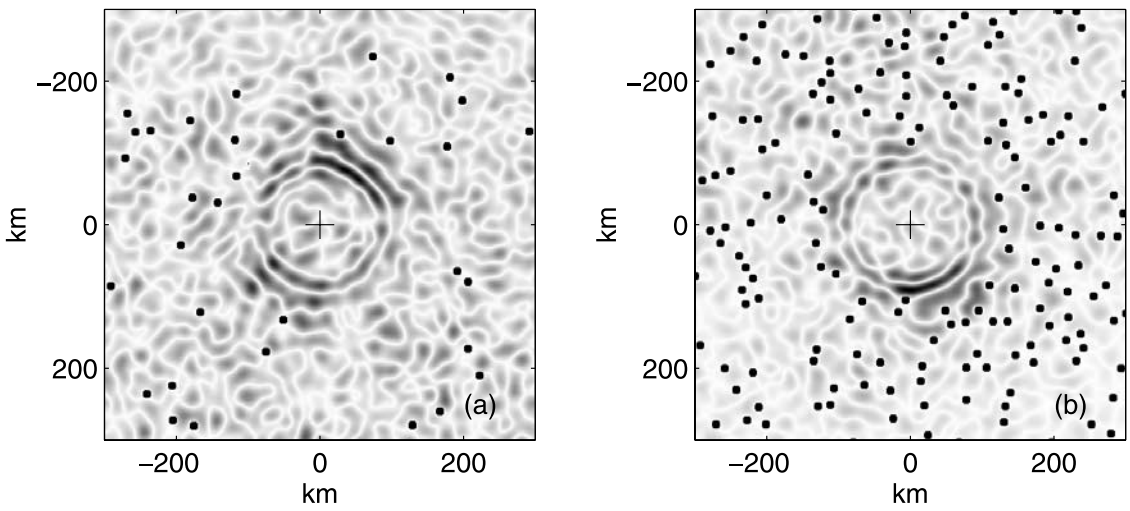

Figure 8. (a) Same experiment as in Figure 7 for time $t = -30$ s in the weakly diffusive medium. Only the late coda was processed, corresponding to lapse times larger than the mean free time. This part of the acoustic signal is made of multiply scattered waves propagating in all directions. The wave front converges to A. Once again diffusion has restored the wave front isotropy and the time symmetry of the Green function. (b) Same experiment as in Figure 7 for time $t = -30$ s for a strongly scattering medium with mean free path $l^* = 120$ km. The converging wave front is isotropic, and therefore the time symmetry of the Green function is restored.

in the southeast of the center of the network as shown by Figure 2. Because of absorption and noise, the coda records are not long enough to reach the isotropy of the diffuse field. The resulting average flux of energy is responsible for the observed time asymmetry of the cross correlation.

[31] Besides the question of the source distribution, the distribution of scatterers can be a source of time asymmetry as well. In the case of an inhomogeneous distribution of scatterers, one may expect preferential directions of arrival of scattered waves. As discussed above, and whatever its origin, such an anisotropy of the energy flow results in a temporal asymmetry of the correlations.

5. Conclusion

[32] The stacked cross correlations between coda records of regional earthquakes in Alaska display propagating deterministic wave trains. We showed numerical simulations of wave propagation to illustrate the principles of the reconstruction of the Green function from field-to-field correlations. An analogy with a time reversal experiment makes more intuitive the interpretation of the reconstruction in terms of physical propagation of the waves. The prominent arrivals that can be identified from the data set correspond to Love and Rayleigh waves as expected for the Green function between two points at the free surface. The emergence of the Green function is clearer at low frequency (0.1–0.3 Hz) than at higher frequency. The reconstructed signals can be observed for positive and negative correlation times which correspond to the causal (retarded) and anticausal (advanced) Green functions expected theoretically. The analysis of correlation functions is thus a proper way to observe the anticausal Green function, usually absent in experiments. However, the correlations exhibit a clear time asymmetry. We propose that it is a consequence of the nonisotropic nature of diffusive wave fields at finite lapse times. To prove this assertion, we studied the relation between the transition toward diffusion and the apparition of stabilization of P to S energy ratio. The numerical experiments with the elastic radiative transfer equation show that the P to S energy ratio stabilizes rapidly, much before the field becomes isotropic. It is nevertheless a good indicator that the field energy is governed by a diffusion equation. The formal state of equipartition is reached only for asymptotically large lapse times when isotropy of the field is achieved. Numerical experiments also show that at finite times, the rupture of time symmetry is related to the uncomplete azimuthal distribution of sources. The relative amplitude of causal and anticausal waves, and its evolution with time, can be used to measure scattering properties of the medium such as transport mean free path. The extraction of Green functions from coda waves makes new types of measurements with seismic waves possible. They can be performed along paths between stations that could not be obtained with the ballistic waves from earthquakes. Therefore they could contribute to improve significantly the resolution of seismic images.

[33] **Acknowledgments.** We are indebted to G. Abers for helping us to access the data of the BEAAR experiment and to all participants in the experiment. R. Weaver made helpful suggestions and stimulating comments. Thanks to B. van Tiggelen, M. Fink, and N. Shapiro for numerous discussions. We acknowledge the constructive remarks of two anonymous reviewers and of the Associate Editor.

References

Abubakirov, I. R., and A. A. Gusev (1990), Estimation of scattering properties of lithosphere of Kamchatka based on Monte-Carlo simulations of record envelope of a near earthquake, *Phys. Earth Planet. Inter.*, *64*, 52–67.

Aki, K. (1969), Analysis of the seismic coda of local earthquakes as scattered waves, *J. Geophys. Res.*, *74*, 615–618.

Aki, K., and B. Chouet (1975), Origin of coda waves: Source, attenuation, and scattering effects, *J. Geophys. Res.*, *80*, 3322–3342.

Beaudoin, B. C., G. S. Fuis, W. D. Mooney, W. Nokleberg, and N. I. Christensen (1992), Thin, low-velocity crust beneath the southern Yukon Tanana terrane, east central Alaska: Results from Trans-Alaska Crustal Transect refraction/wide-angle reflection data, *J. Geophys. Res.*, *97*, 1921–1942.

Campillo, M., and A. Paul (2003), Long-range correlations in the diffuse seismic coda, *Science*, *299*, 547–549.

Campillo, M., L. Margerin, and N. M. Shapiro (1999), Seismic wave diffusion in the Earth lithosphere, in *Diffuse Waves in Complex Media*, *NATO ASI Ser., Ser. C*, vol. 531, edited by J. P. Fouque, pp. 383–404, Springer, New York.

Derode, A., A. Tourin, and M. Fink (1999), Ultrasonic pulse compression with one-bit time reversal through multiple scattering, *J. Appl. Phys.*, *85*, 6343–6352.

Derode, A., M. Tanter, L. Sandrin, A. Tourin, and M. Fink (2001), Numerical and experimental time-reversal of acoustic waves in random media, *J. Comput. Acoust.*, *9*(3), 991–998.

Derode, A., E. Larose, M. Tanter, J. de Rosny, A. Tourin, M. Campillo, and M. Fink (2003a), Recovering the Green's function from field-field correlations in an open scattering medium (L), *J. Acoust. Soc. Am.*, *113*, 2973–2976.

Derode, A., E. Larose, M. Campillo, and M. Fink (2003b), How to estimate the Green's function of a heterogeneous medium between two passive sensors? Application to acoustic waves, *Appl. Phys. Lett.*, *83*, 3054–3056.

Duvall, T. L., S. M. Jefferies, J. W. Harvey, and M. A. Pomerantz (1993), Time distance helioseismology, *Nature*, *362*, 430–432.

Ferris, A., G. A. Abers, D. H. Christensen, and E. Veenstra (2003), High resolution image of the subducted Pacific(?) plate beneath central Alaska, 50–150 km depth, *Earth Planet. Sci. Lett.*, *214*, 575–588.

Fink, M. (1992), Time reversal of ultrasonic fields-Part I: Basic principles, *IEEE Trans. Ultrason. Ferroelectr. Frequation Control*, *39*(5), 555–566.

Hennino, R., N. Tregoures, N. M. Shapiro, L. Margerin, M. Campillo, B. A. van Tiggelen, and R. L. Weaver (2001), Observation of equipartition of seismic waves, *Phys. Rev. Lett.*, *86*, 3447–3450.

Hoshiba, M. (1991), Simulation of multiple scattered coda wave excitation based on the energy conservation law, *Phys. Earth Planet. Inter.*, *67*, 123–136.

Lacombe, C., M. Campillo, A. Paul, and L. Margerin (2003), Separation of intrinsic absorption and scattering attenuation from Lg coda decay in central France, *Geophys. J. Int.*, *154*, 417–425.

Larose, E., A. Derode, M. Campillo, and M. Fink (2004), Imaging from one-bit correlations of wideband diffuse wave fields, *J. Appl. Phys.*, *95*, 8393–8399.

Lobkis, O. I., and R. L. Weaver (2001), On the emergence of the Green's function in the correlations of a diffuse field, *J. Acoust. Soc. Am.*, *110*, 3011–3017.

Malcolm, A. E., J. Scales, and B. A. van Tiggelen (2004), Extracting the Green function from diffuse, equipartitioned waves, *Phys. Rev. E*, *70*, 015601.

Margerin, L., M. Campillo, and B. van Tiggelen (1998), Radiative transfer and diffusion of waves in a layered medium: New insight on coda Q, *Geophys. J. Int.*, *134*, 596–612.

Margerin, L., M. Campillo, N. M. Shapiro, and B. van Tiggelen (1999), Residence time of diffuse waves in the crust as a physical interpretation of coda Q: Application to seismograms recorded in Mexico, *Geophys. J. Int.*, *138*, 343–352.

Margerin, L., M. Campillo, and B. van Tiggelen (2000), Multiple scattering of elastic waves, *J. Geophys. Res.*, *105*, 7873–7892.

Rickett, J. E., and J. F. Claerbout (2000), Calculation of the Sun's impulse response by multi-dimensional spectral factorization, *Sol. Phys.*, *192*, 203–210.

Ryzhik, L., G. Papanicolaou, and J. B. Keller (1996), Transport equations for elastic and other waves in random media, *Wave Motion*, *24*, 327–370.

Shapiro, N. M., and M. Campillo (2004), Emergence of broadband Rayleigh waves from correlations of the ambient seismic noise, *Geophys. Res. Lett.*, *31*, L07614, doi:10.1029/2004GL019491.

Shapiro, N. M., M. Campillo, L. Margerin, S. K. Singh, V. Kostoglodov, and J. Pacheco (2000), The energy partitioning and the diffusive character of the seismic coda, *Bull. Seismol. Soc. Am.*, *90*, 655–665.

Snieder, R. (2004), Extracting the Green's function from the correlation of coda waves: A derivation based on stationary phase, *Phys. Rev. E*, *69*, 046610.

Tanter, M. (1999), Application of time reversal to brain hyperthermia, Ph.D thesis, Univ. Paris VII, Paris.

Turner, J. A. (1998), Scattering and diffusion of seismic waves, *Bull. Seismol. Soc. Am.*, *88*, 276–283.

van Tiggelen, B. A. (2003), Green function retrieval and time reversal in a sisordered world, *Phys. Rev. Lett.*, *91*, 243904.

Wapenaar, K. (2004), Retrieving the elastodynamic Green's function of an arbitrary inhomogeneous medium by cross correlation, *Phys. Rev. Lett.*, *93*, 254301.

Weaver, R. L. (1982), On diffuse waves in solid media, *J. Acoust. Soc. Am.*, *71*, 1608–1609.

Weaver, R. L. (1985), Diffuse elastic waves at a free surface, *J. Acoust. Soc. Am.*, *78*, 131–136.

Weaver, R. L. (1990), Diffusivity of ultrasound in polycrystals, *J. Mech. Phys. Solids*, *38*, 55–86.

Weaver, R. L., and O. I. Lobkis (2001), Ultrasonics without a source: Thermal fluctuation correlation at MHz frequencies, *Phys. Rev. Lett.*, *87*, 134301.

Weaver, R. L., and O. I. Lobkis (2002), On the emergence of the Green's function in the correlations of a diffuse field: Pulse-echo using thermal phonons, *Ultrasonics*, *40*, 435–439.

Weaver, R. L., and O. I. Lobkis (2004), Diffuse fields in open systems and the emergence of the Green's function, *J. Acoust. Soc. Am.*, *116*, 2731–2734.

Wu, F., J.-L. Thomas, and M. Fink (1992), Time reversal of ultrasonic fields–part II: Experimental results, *IEEE Trans. Ultrason. Ferroelectr. Frequation Control*, *39*(5), 567–578.

M. Campillo, E. Larose, L. Margerin, and A. Paul, Laboratoire de Géophysique Interne et Tectonophysique, Observatoire de Grenoble, Université Joseph Fourier and CNRS, BP 53, F-38041 Grenoble, France. (anne.paul@obs.ujf-grenoble.fr)

A. Derode, Laboratoire Ondes et Acoustique, Université Paris 7 and CNRS, ESPCI, 10 rue Vauquelin, F-75005 Paris, France.